Framework for replacing steel with aluminum fibers in bituminous mixes

N. G. Pavlatos[1], P. Apostolidis[1] & A. Scarpas[2]
[1]*Section of Pavement Engineering, Faculty of Civil Engineering and Geosciences, Delft University of Technology, Delft, The Netherlands.*

[2]*Department of Civil Infrastructure and Environmental Engineering, Khalifa University of Science and Technology, Abu Dhabi, United Arab Emirates*

ABSTRACT: This research explores the incentives for replacing steel fibers with aluminum fibers in fiber modified bituminous mixes. In this work the focus is on fiber modified bituminous mixes especially designed for induction heating. Inductive fibers are heated up because eddy currents are generated - according to Joule's law - when alternating magnetic field is applied by electro-magnetic induction coil. Aluminum fiber-type particles are proposed as an alternative solution for developing corrosion resistant and lightweight bituminous mixes capable to be induced by electro-magnetic fields. In another publication (Pavlatos et al., Inductive bituminous mortar with steel and aluminum fibers, *Advances in Materials and Pavement Performance Prediction*, Submitted, 2018), a finite element three-dimensional model is developed in order to determine the effective electrical conductivity of steel and aluminum fiber modified bituminous mortar, as well as to show the potential utilization of alternative particles for developing multi-functional paving materials with improved properties.

1. INTRODUCTION

Bituminous mixes are widely used in the construction industry mainly for the transportation infrastructure and are non-inductive materials. However, when inductive steel particles (i.e., steel fibers, steel slag, etc.) are added they become suitable for electro-magnetic induction (Garcia et al.; 2009, Liu et al., 2012; Apostolidis et al., 2016a). These materials can be heated locally under a time-variable magnetic field. Particularly, the magnetic field induces eddy currents in particles within the bituminous matrix - according to Faraday's law - and they are heated up based on the principles of Joule's law. The generated heat in the particles increases the temperature and through the temperature rise the viscosity of the bituminous part of the mix is being reduced, the micro-cracks are closing and eventually mechanical properties are recovered. However, the addition of inductive particles into conventional paving materials substantially increases the total weight of plant-produced bituminous mixes, thus resulting in higher production and transportation costs in the manufacturing chain of inductive pavements. Moreover, the environmental conditions that the pavement is exposed to during its service life result in corrosion of the steel fibers and therefore the long-term performance of inductive bituminous mixes is adversely affected. The corrosion and weight issues in fiber modified bituminous mixes are described in detail in the next sub-sections.

2. CORROSION BEHAVIOUR IN INDUCTIVE BITUMINOUS MIXES

The main component of ordinary carbon steel fibers is iron (Fe) which is very susceptible to corrosion. Iron in bituminous pavements comes in contact with water and oxygen, resulting in the ordinary red/brown rust (Bardal, 2014). The resulting rust can be seen in Figure 1 which is from ongoing research that takes place at Delft University of Technology (Apostolidis et al., 2016b). More irregular types of corrosion - e.g. black rust - are not considered in this paper for simplicity and because they are less likely to occur in pavements.

Figure 1. Corroded steel fibers in bituminous concrete samples

The corrosion of steel fibers in bituminous mixes can be interpreted as many small differential aeration cells. Water drops (moisture in general) which are in contact with steel fiber exhibit an oxygen concentration gradient. The oxygen concentration is high close to the outer exposed surface of the water drop because the supply of oxygen is easy, whereas oxygen concentration is lower inside the water drop because the supply of

oxygen is harder. This oxygen concentration gradient produces a cathodic and an anodic site where reduction and oxidation take place respectively; reduction of oxygen occurs close to the exposed water drop surface (cathode), while oxidation of iron takes place inside the water drop (anode). The electrons move from the anodic (oxidation) region to the cathodic (reduction) region via the metal. Equation 1 and Equation 2 describe the anodic and cathode reactions that take place (Brown et al., 2014).

$$Cathode:\ O_2(g)+4H^+(aq)+4e^- \xrightarrow{red.} 2H_2O(l) \quad (1)$$

$$Anode:\ Fe(s) \xrightarrow{oxid.} Fe^{2+}(aq)+2e^- \quad (2)$$

The reduction of oxygen consumes protons existing in the water drop. Therefore, by considering the autoionization of water under Le Chatelier's principle, the chemical equilibrium of the autoionization reaction will shift to the right. This equilibrium shift creates an environment rich in hydroxide anions. The dissolved iron cation reacts with the hydroxide anion to form iron(II) hydroxide. The iron(II) hydroxide further reacts with the environment where the iron is once again oxidized and hydrated iron(III) oxide is formed. The latter is the reddish-brownish solid that is often referred to as rust. This process is described in Equation 3, Equation 4 and Equation 5. The entire corrosion process is visualized in Figure 2.

$$H2O(l) \rightleftharpoons H^+(aq)+OH^-(aq) \quad (3)$$

$$Fe^{2+}(aq)+2OH^-(aq) \longrightarrow Fe(OH)_2(s) \quad (4)$$

$$4Fe(OH)_2(s)+O_2(g)+xH_2O(l) \longrightarrow 2Fe_2O_3(x+4)H_2O(s) \quad (5)$$

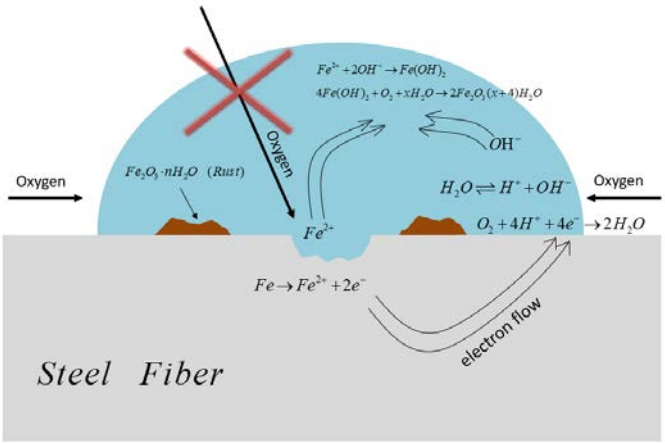

Figure 2. Corrosion process of steel fibers

When it comes to corrosion concerns, aluminum could be initially considered as a bad candidate since according to thermodynamics it is a very reactive metal with low corrosion resistance (Hatch, 1984). As a comparison, the standard reduction potential of iron versus the standard hydrogen electrode is -0.447 V, whereas the standard reduction potential of aluminum versus the standard hydrogen electrode is -1.676 V (Haynes 2016). However, when a freshly created aluminum surface is exposed to the atmosphere a thin oxide "skin" is formed. The oxide layer, which is only a few nanometers thick, is of greater importance in many applications as it protects the underlying metal from further oxidation. This self-protecting characteristic gives aluminum its surprisingly high resistance to corrosion (Davis, 1999). The aluminum can be under passivation in pH ranging from 4.0 to 8.5 according to the Pourbaix diagram in Figure 3 (Pourbaix 1966). This pH range ensures the thermodynamic stability of the protective oxide layer. Rigorous studies of pavement runoff and highway drainage waters suggest that there is a small variation in the pH values with an average value of ~7.4 (Harrison and Wilson 1985; Sansalone et al. 1996). Even when the quality of road runoff at a highly trafficked road was monitored for 2 years, the pH only exhibited a small range between 6.2 and 8.3 with a median and mean value of 7.5 (Helmreich et al. 2010). Furthermore, extensive studies of the rainwater pH (Rao et al. 2017; Uchiyama et al. 2017) suggest that the pavement will not be exposed to pH outside the passive region of aluminum as a consequence of future rainfalls.

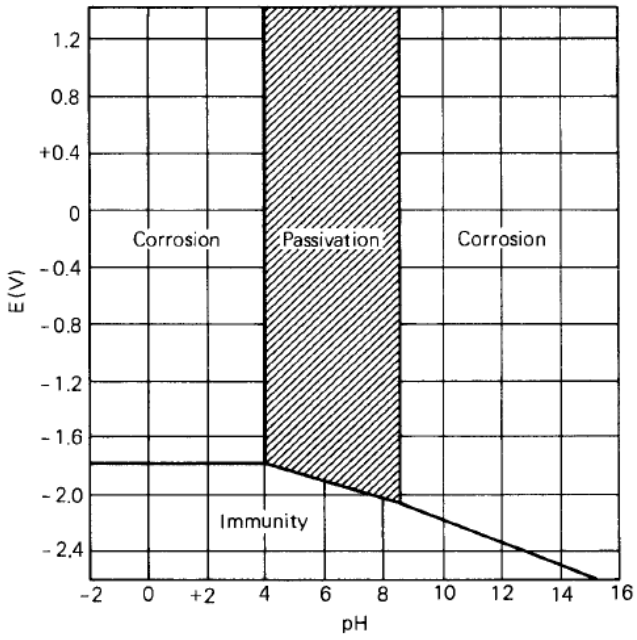

Figure 3. Pourbaix diagram for aluminum

The different behavior of steel and aluminum fibers with respect to corrosion - assuming

conditions typical for a pavement - can be summarized in Figure 4.

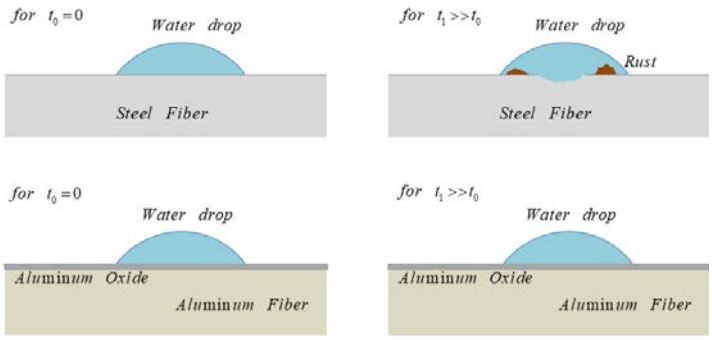

Figure 4. Steel versus aluminum fiber corrosion behavior

3. WEIGHT OF INDUCTIVE BITUMINOUS MIXES

When it comes to using steel fibers in inductive bituminous mixes and asphalt concrete, corrosion is not the only issue. A major complaint of the industry is the additional weight that is introduced with the addition of steel fibers. The hot mix asphalt (HMA) is typically transported from the plant to the construction site by trucks. The transportation of the HMA is governed by 2 limiting factors; the volume capacity of the truck and the weight capacity of the truck. Throughout the years the truck design has been optimized so that when a truck is fully loaded then it can safely carry the weight but without much margin left. However, this is true for ordinary mixes that consist of mineral particles, binder and air voids with typical densities of d_{mp} = 2700 kg/m^3, d_{bin} = 1020 kg/m^3 and d_{air} = 0 kg/m^3 respectively. The situation changes when steel fibers are added with typical density d_{sf} = 7800 kg/ m^3 = 2.89d_{mp} = 7.65d_{bin} (ASM International 1990a). As a result, the trucks hit their weight limit before fully loaded. This is translated to inefficiency, additional transportation trips, additional costs and further project delays. Moreover, the increase in the number of trips transporting HMA from the plant to the site introduces extra project risk since it increases the chance that the trucks with HMA will face more traffic and delays than accounted for.

To provide a better illustration of the issue, a cubic meter of a hypothetical HMA is examined with volume fraction for mineral particles V_{mp} = 86%, volume fraction for binder V_{bin} = 8% and volume fraction of air voids V_{air} = 6%. By using the typical density values stated earlier in this paper the total mass of the cubic meter of HMA M_{tot} = 2403.6 kg can be calculated. The phase diagram for the hypothetical asphalt concrete is presented in Figure 5. Then we consider that the same HMA basis contains steel fibers and the volume fraction of steel fibers is V_{sf} = 2.5%. The updated volume fractions for mineral particles, binder and air voids are V_{mp} = 83.85%, V_{bin} = 7.8% and V_{air} = 5.85% respectively. By using the typical densities stated previously in this paper the total mass of the cubic meter of HMA with steel fibers $M_{tot,sf}$ = 2538.51 kg can be calculated. This results in a mass increase of 5.62% compared to HMA without steel fibers. The phase diagram for the hypothetical asphalt concrete with steel fibers is presented in Figure 6. If we consider the fibers to be aluminum, then the updated volume fractions for mineral particles, binder, aluminum fibers and air voids are V_{mp} = 83.85%, V_{bin} = 7.8%, V_{sf} = 2.5% and V_{air} = 5.85% respectively. Using a typical density d_{af} = 2700 kg/ m^3 for aluminum fibers (ASM International 1990b) and the typical densities stated earlier in this paper for the other components, the total mass of the cubic meter of HMA with aluminum fibers $M_{tot,af}$ = 2411.01 kg can be calculated. This value is 5.29% lower than HMA with steel fibers and a mere 0.31% higher than the HMA without any fibers. The phase diagram for the hypothetical asphalt concrete with aluminum fibers is presented in Figure 7.

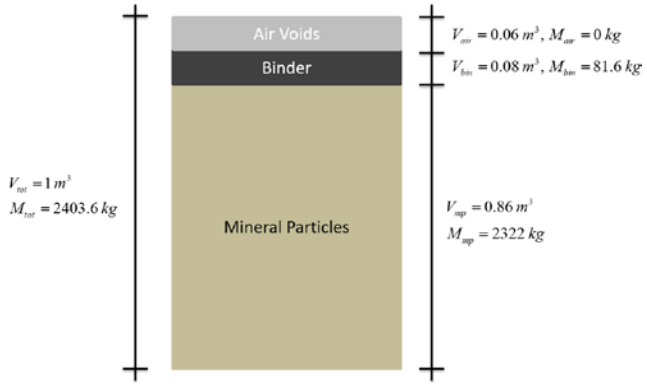

Figure 5. Phase diagram for HMA

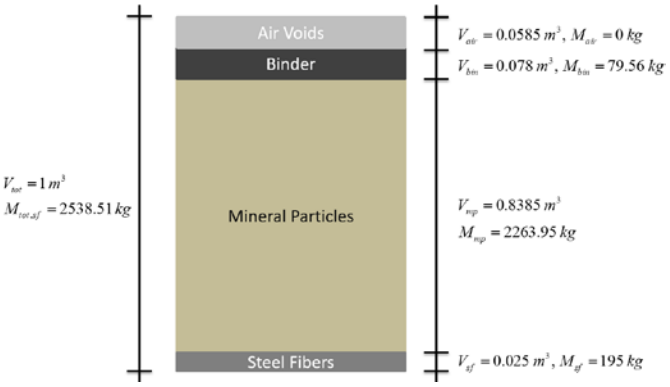

Figure 6. Phase diagram for HMA with steel fibers

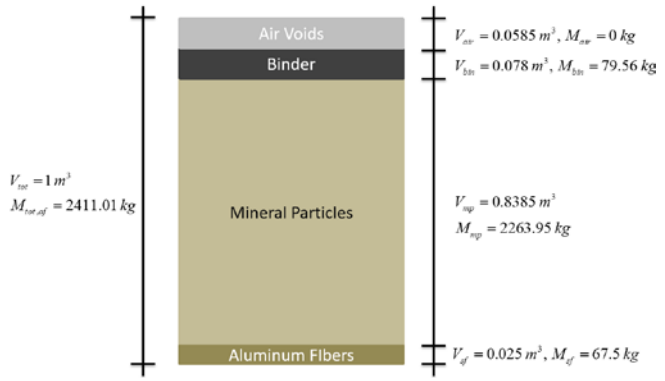

Figure 7. Phase diagram for HMA with aluminum fibers

4. CONCLUSIONS & RECOMMENDATIONS

In this paper we suggested the use of aluminum fibers in inductive bituminous mixes instead of steel fibers. We examined the corrosion mechanisms and the aluminum fibers can be viewed as a superior choice to steel fibers. Moreover, we presented an example that demonstrates the weight increase of HMA when steel fibers are added and how this can be avoided with aluminum fibers. We suggest further research, both modeling and experimental, to demonstrate that aluminum fibers can be used as an alternative to steel fibers for induction heating of bituminous mixes, and perhaps even achieve induction heating with higher efficiency.

REFERENCES

Apostolidis P., Liu X., Scarpas A., Kasbergen C. & van de Ven. M., 2016a. Advanced Evaluation of Asphalt Mortar for Induction Healing Purposes. *Construction and Building Materials* 126, 9-25.

Apostolidis P., Liu X., Scarpas A., van de Ven M. & van Bochove G., 2016b. Evaluation of Chloride Induced Damage in Stone Mastic Asphalt Mixes Suitable for Induction Heating. *Functional Pavement Design - Erkens et al. (eds). 2016 Taylor & Francis Group*, London, at Delft, The Netherlands.

ASM International Handbook Committee, 1990a. *Volume 1, Properties and Selection: Irons, Steels, and High-Performance Alloys*. ASM International, 10th Edition.

ASM International Handbook Committee, 1990b. *Volume 2, Properties and Selection: Nonferrous Alloys and Special-Purpose Materials*. ASM International, 10th Edition.

Bardal E., 2004. *Corrosion and Protection*. Springer, 1st Edition.

Brown T.L., LeMay H.E., Bursten B.E., Murphy C.J., Woodward P.M. & Stoltzfus M.W., 2014. *Chemistry: The Central Science*. Pearson, 13th Edition.

Davis J. R., 1999. *Corrosion of Aluminum and Aluminum Alloys*. ASM International, 1st Edition.

Garcia A., Schlangen E., van de Ven M. & Liu Q., 2009. Electrical Conductivity of Asphalt Mortar Containing Conductive Fibers and Fillers. *Construction and Building Materials* 23, 3175-3181.

Harrison R. M. & Wilson S. J., 1985. The Chemical Composition of Highway Drainage Waters I. Major Ions and Selected Trace Metals. *The Science of the Total Environment* Vol. 43, Issues 1-2, 63-67.

Hatch J. E., 1984. *Aluminum Properties and Physical Metallurgy*. ASM International, 1st Edition.

Haynes W. M., 2016. *CRC Handbook of Chemistry and Physics*. CRC Press, 97th Edition.

Helmreich B., Hilliges R., Schriewer A. & Horn H. 2010. Runoff Pollutants of a Highly Trafficked Urban Road – Correlation Analysis and Seasonal Influences. *Chemosphere* Vol. 80, Issue 9, 991-997.

Liu G., Schlangen E. & van de Ven M., 2012. Induction Healing of Porous Asphalt Concrete. *Transportation Research Record*, 2305, TRB, National Research Council, Washington, D.C., 95-101.

Pavlatos N.G., Apostolidis P., Scarpas A., Liu X. & van de Ven M., 2018. Inductive Bituminous Mortar with Steel and Aluminum Fibers, *Advances in Materials and Pavement Performance Prediction*, Submitted.

Pourbaix M., 1966. *Atlas of Electrochemical Equilibria in Aqueous Solution*. Oxford; New York: Pergamon Press.

Rao W., Han G., Tan H., Jin K., Wang S. & Chen T., 2017. Chemical and Sr Isotopic Characteristics of Rainwater on the Alxa Desert Plateu, North China: Implication for Air Quality and Ion Sources. *Atmospheric Research* Vol. 193, 163-172.

Sansalone J. J., Buchberger S. G. & Al-Abed S. R., 1996. Fractionation of Heavy Metals in Pavement Runoff. *The Science of the Total Environment* Vol. 189-190, 371-378.

Uchiyama R., Okochi H., Ogata H., Katsumi N. & Asai D., 2017. Geochemical and Stable Isotope Characteristics of Urban Heavy Rain in the Downtown of Tokyo, Japan. *Atmospheric Research* Vol. 194, 109-118.